Spectral Unmixing of Multispectral Satellite Images with Dimensionality Expansion Using Morphological Profiles

Sergio Bernabé[a,c], Prashanth Reddy Marpu[b], Antonio Plaza[a] and Jon Atli Benediktsson[c]

[a]Hyperspectral Computing Laboratory
University of Extremadura, Cáceres, SPAIN
E-mail: sergiobernabe, aplaza@unex.es
[b]Masdar Institute of Science and Technology
Abu Dhabi, UAE
E-mail: prashanthmarpu@ieee.org
[c]Faculty of Electrical and Computer Engineering
University of Iceland, Reykjavik, ICELAND
E-mail: benedikt@hi.es

ABSTRACT

In this paper, we develop a new framework for spectral unmixing of multispectral remote sensing images with limited spectral resolution. Our proposed approach performs dimensionality expansion by taking advantage of the spatial information contained in such images. For this purpose, in this work, we experiment with morphological profiles and morphological attribute filters, which allow expanding the dimensionality of the original image and obtaining a detailed signature (profile) at each pixel using the SVM classifier. This allows for the application of spectral unmixing techniques that integrate both the spatial and the spectral information, since the unmixing is not only based on the original multispectral/color information but also takes into account the additional bands included by exploiting the spatial information. The unmixing chain considered in this work comprises a classic endmember extraction algorithm: vertex component analysis (VCA) followed by fully constrained linear spectral unmixing (FCLSU) to estimate the abundance of each endmember in each pixel of the image. Kernel principal component analysis (KPCA) is also used in the considered chain, to increase dimensionality in the spectral domain only and to perform feature extraction. In order to quantitatively validate the proposed framework, we use the RGB bands of a set of registered hyperspectral images. Specifically, we use the ground-truth to validate the unmixing results obtained for the lower spatial resolution scenes. Our experimental results indicate that the proposed dimensionality expansion strategy allows for the successful unmixing of multispectral satellite images, specially for RGB/color images.

Keywords: Spectral unmixing, multispectral satellite images, endmember extraction

1. INTRODUCTION

Spectral unmixing aims to estimate the abundance of macroscopically pure components (often called endmembers in spectral unmixing terminology) within each pixel observation. One of the main methodological requirements for spectral unmixing is the availability of rich information in the spectral domain, i.e. the images to be unmixed should have at least as many bands as the number of endmembers to be identified. Unfortunately, there is a vast amount of remote sensing data in which the number of spectral bands is not as high as the number of distinct components or endmembers. This is the case for multispectral or color satellite images, which only comprise a few bands and, hence, cannot accommodate a large number of spectral endmembers. As a result, the application of spectral unmixing techniques to these remote sensing images has been limited by dimensionality issues, even if there is enough information to identify distinct spectral components of different types of materials.

Utilization of spatial information for unmixing of hyperspectral images has already been proposed in literature. Morphological filters were used by Plaza et al.[1] and watershed transformation was used by Zortea and Plaza[2] to identify the best endmembers from spatially homogenous regions. MRFs are used by Eches et al.[3] to model the spatial information in the Bayesian framework for spectral unmixing. A fuzzy local information proportion

Satellite Data Compression, Communications, and Processing VIII,
edited by Bormin Huang, Antonio J. Plaza, Carole Thiebaut, Proc. of SPIE Vol. 8514,
85140Z · © 2012 SPIE · CCC code: 0277-786X/12/$18 · doi: 10.1117/12.930418

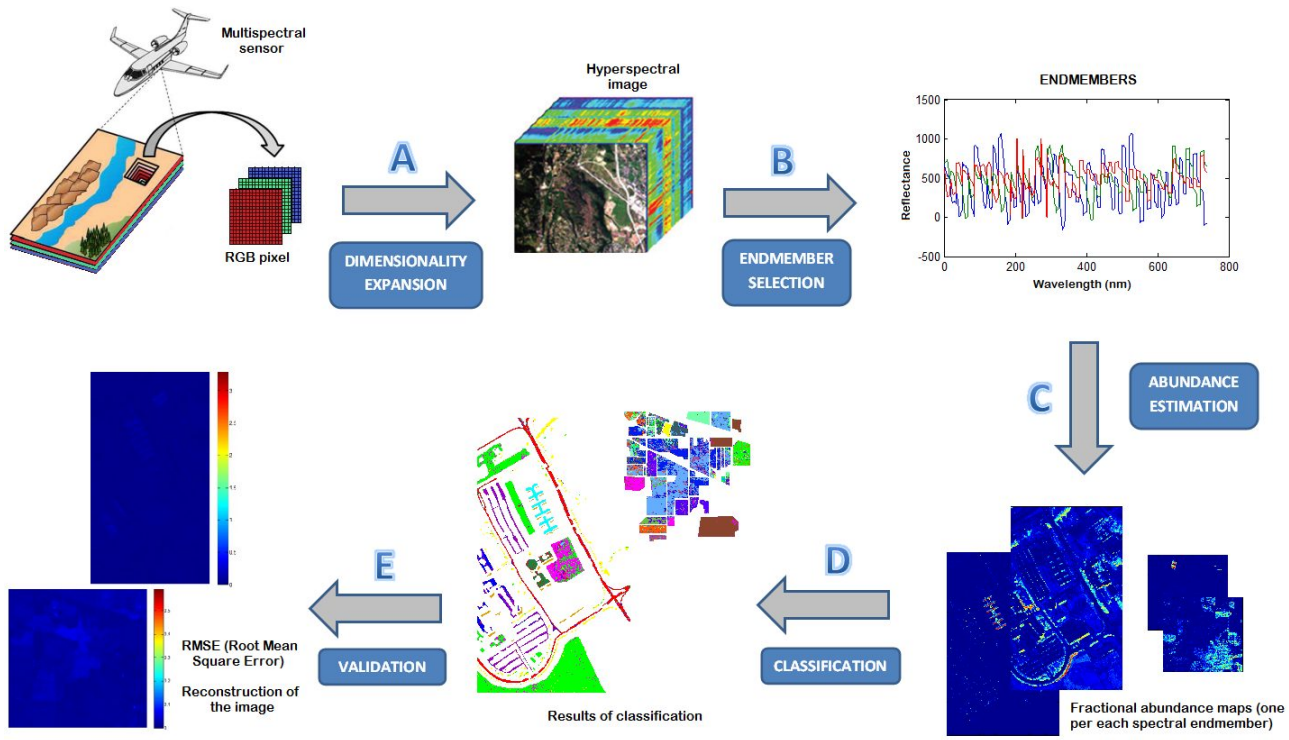

Figure 1. Block diagram illustrating the complete process for a new unmixing chain improvements on the dimensionality expansion on a RGB image and validation.

estimation algorithm is presented by Zare[4] where the spatial information is added as a regularization term in the optimization problem. A total variation regularization term is introduced in the sparse regression problem in the method proposed by Iordache et al.[5] Spatial information is also used by Villa et al.[6] to increase the spatial resolution of the resulting maps by means of spectral unmixing. However spectral unmixing of multispectral images has not been studied in detail. We propose to use the concept of morphological attribute profiles[7] to fuse the spatial information and increase the dimensionality of the data. The obtained endmembers may not have physical meaning like the spectral endmembers of the hyperspectral data, but they might have some correlation to the spatial characteristics of the objects. Furthermore, experiments are also carried out to test the usage of Kernel Principal Component Analysis (KPCA) to expand the dimensionality of the RGB images.

The paper is organized in five sections. The next section explain a new spectral unmixing methodology used to improve spatial and spectral information of RGB images and achieve better classification results. Section 3, morphological attribute profiles are formally defined. Section 4 presents the results of the experimental analysis carried out for assessing the effectiveness of our proposed unmixing chain. Finally, conclusions are drawn in Section 5.

2. SPECTRAL UNMIXING METHODOLOGY

In this section, we describe the methodology used to design an unmixing-based feature extraction chain on RGB/color images which can be summarized by the flowchart in Fig. 1. The process chain is divided into five steps:

A) The first step consists in the dimensionality expansion of the RGB image. In this step, we can either use only spectral information or both spetral and spatial information to get a new expanded image. In this work, we have used the Kernel Principal Component Analysis (KPCA) for spectral information only and the Extended Multi-Attribute Attribute Profiles (EMAPs)[8] for spectral-spatial information.

B) In this step, we estimate the number of endmembers p directly from the expanded $n-$dimensional image **I**. For this purpose, we use the virtual dimensionality (VD) concept[9] in this work which is a standard technique widely used in the literature. Once the number of endmembers p has been estimated, we apply an automatic algorithm to extract a set of endmembers from the expanded image. In this case, we have selected the vertex component analysis (VCA) algorithm,[10] which shown very similar results in terms of computational time to obtan it and accuracy conducted with other endmember extraction techniques in previous work.

C) The third step in the unmixing chain applies a fully ASC-constrained and ANC-constrained linear spectral unmixing (is referred to by the acronym FCLSU[11]) to estimate the fractional coverage of each endmember in each pixel of the expanded image, providing a set of p abundance maps. In this step, we obtain one fractional abundance map per each spectral endmember.

D) In the next step of the complete unmixing chain, the standard support vector machine (SVM) classification is performed on the stack of abundance fractions using randomly selected training samples (i.e. 5%, 10%, of the available samples per class).

E) The last step consists in the validation of the classification results to verify the goodness of our proposed complete unmixing chain. The metric employed to evaluate the goodness of the reconstruction is the root mean square error (RMSE) obtained in the reconstruction of the expanded image (using the derived endmembers and their corresponding abundance fractions). The expanded image is used to measure the fidelity of the reconstructed version of the same scene on a per-pixel basis.

3. MORPHOLOGICAL ATTRIBUTE PROFILES

The concepts of Morphological Profiles (MPs)[12] and Attribute Profiles (APs)[7,8] have been successfully employed for combining the spectral and spatial information while classifying remote sensing imagery. AP is obtained by applying a sequence of Attribute Filters (AFs) to a gray level image.[7] AFs are operators defined in the mathematical morphology framework which operate by merging connected components at different levels in the image.[13] Extended Attribute Profiles (EAPs)[8] are an extension of APs for the analysis of multi/hyper-spectral images. The EAP is a stack of APs obtained with different features. When the EAPs obtained using different types of attributes are stacked together, the resulting profile is called as Extended Multi-Attribute Attribute Profile (EMAP).[8]

The filtering operation is based on the evaluation of how an attribute a computed for every region, compares to a given reference value λ. For a connected component of the image, C_i, if $a(C_i) > \lambda$, then the region is kept unaltered, otherwise it is set to the grayscale value of the adjacent region with closer value, thereby merging the connected components. When the region is merged to the adjacent region of a lower (or greater) gray level, the operation performed is a thinning (or thickening).

Given a sequence of thresholds $\lambda = \lambda_1, \lambda_2, \cdots, \lambda_n$, an AP is obtained by applying a sequence of attribute thinning and attribute thickening operations to the input image f, see eq. 1,

$$\mathrm{AP}(f) = \{\phi_n(f), \cdots, \phi_1(f), \mathrm{f}, \gamma_1(f), \cdots, \gamma_n(f)\} \tag{1}$$

where ϕ_i and γ_i are the thickening and thinning transformations respectively.

The EAP (eq. 2), is obtained by generating an AP on each of the first m features (F_i) computed using any feature reduction technique on the multi/hyperspectral image:[8]

$$\mathrm{EAP} = \{\mathrm{AP}(\mathrm{F}_1), \mathrm{AP}(\mathrm{F}_2), \cdots, \mathrm{AP}(\mathrm{F}_m)\} \tag{2}$$

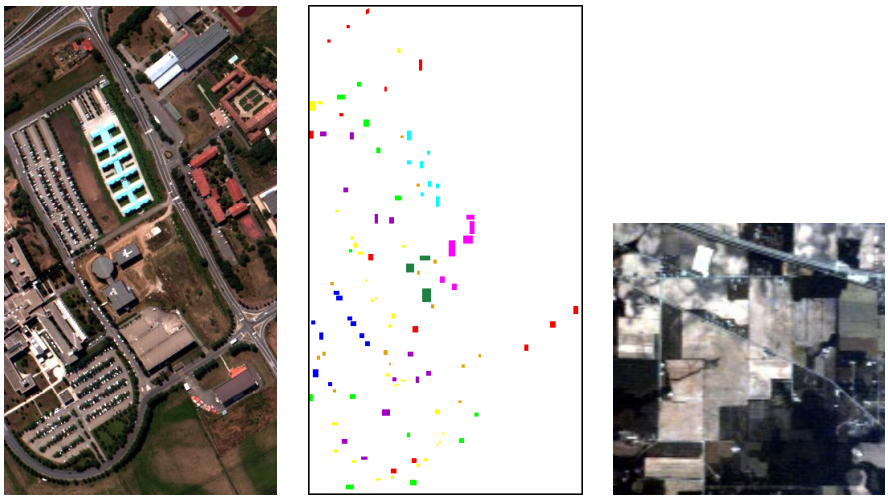

(a) (b) (c)

Figure 2. (a) RGB composite of the hyperspectral ROSIS Pavia scene. (b) Training set commonly used for the ROSIS Pavia scene. (c) RGB composite of the hyperspectral Indian Pines scene.

4. EXPERIMENTAL RESULTS

In this section, we present a quantitative and comparative analysis of different feature extraction techniques for hyperspectral image classification, including unmxing-based approaches with reference to RGB and hyperspectral images. The main goal is to use spectral unmixing techinques in multispectral images so that we can validate the classification results using EMAP and dimensionality expansion with some kind of metric employed to evaluate the goodness of the reconstruction such as the root mean square error (RMSE). The combination of these techniques provides a data processing approach that has not been explored in previous constributions. Before describing the results obtanied in experimental validation, we first describe the data set and experimental setup used in our experiments. Then, in Section 4.3 the obtained classification results will be analyzed with the different feature extraction techniques. Finally, Section 4.4 discusses the obtained results to evaluate the reconstruction for each image from the data obtained with different feature extraction techinques used in this work.

4.1 Data Set Description

The experimental analysis was carried out by clasifying two images corresponding to different scenes acquired using two different sensors: AVIRIS, ROSIS. The images span a wide range of land cover types e.g., agricultural areas of Indian Pines and urban zones in the town of Pavia. In the following, we briefly describe each of the data sets considered in our study.

4.1.1 ROSIS Pavia

The first data set used in our experiments was acquired using the ROSIS optical sensor over the urban area of the University of Pavia, Italy. The image size in pixels is 640×340, with high spatial resolution of 1.3 meters per pixel. The number of data channels in the acquired image is 115 (with spectral range from 0.43 to 0.86 μm). Fig. 2 (a) shows a RGB composite of the hyperspectral image used in this work, while Fig. 4 (a) shows nine ground-truth classes of interest, which comprise urban features, as well as soil and vegetation features. Finally, Fig. 2 (b) shows a commonly used training set directly derived from the ground-truth in Fig. 4 (a).

4.1.2 AVIRIS Indian Pines

The second data set used in our experiments was acquired using the AVIRIS sensor over the Indian Pines region in Northwestern Indiana in 1992. This scene, with a size of 145 lines by 145 samples, was acquired over a mixed agricultural/forest area, early in the growing season. The scene comprises 202 spectral channels (with spectral range from 0.4 to 2.5 μm, nominal spectral resolution of 10 nm, moderate spatial resolution of 20 meters by pixel, and 16-bit radiometric resolution). Fig. 2 (c) shows a RGB composite of the hyperspectral image used in

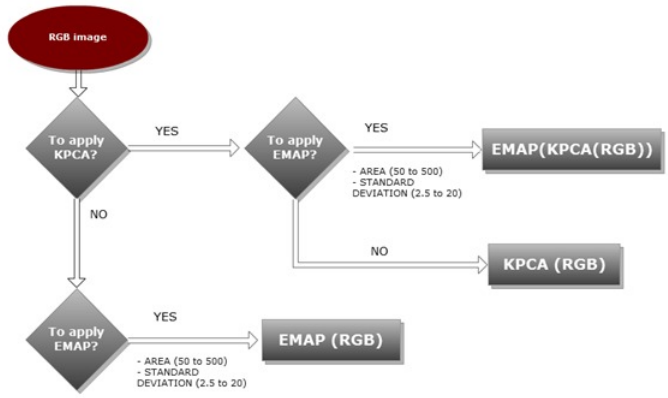

Figure 3. Flowchart with the differents experimental setup using EMAP, KPCA and KPCA+EMAP.

Table 1. Overall accuracy (in percentage) and standard deviation obtained after aplying the differents unmixing chains with the SVM classifier for the PAVIA UNIVERSITY scene.

Overall Accuracy	**ROSIS PAVIA UNIVERSITY**		
Features	**Standard**	**50 pixels**	**5% Training**
RGB Multispectral	65.81% ± 0.00	62.67% ± 5.62	78.87% ± 0.40
Original Hyperspectral	70.25% ± 1.85 (13)	70.01% ± 2.38 (13)	83.48% ± 1.33 (13)
EMAP(RGB)	72.25% ± 3.39 (13)	73.78% ± 4.19 (13)	85.65% ± 1.86 (13)
KPCA(RGB)	65.09% ± 2.91 (13)	63.18% ± 3.40 (13)	77.34% ± 0.57 (13)
EMAP(KPCA(RGB))	**74.16% ± 2.19 (13)**	**74.50% ± 3.29 (13)**	**86.60% ± 1.01 (13)**

our experiments, while Fig. 5 (a) shows the ground-truth map available for the scene, displayed in the form of a class assignment for each labeled pixel, with 16 mutually exclusive ground-truth classes. These data, including ground-truth information, are available online*.

4.2 Experimental Setup

The EMAP is built using the area (related the size of the regions) and standard deviation (with measures the homogeneity of the pixels enclosed by the regions) attributes with threshold values of 50 to 500 and 2.5 to 20 respectively. For KPCA, 2000 pixels were considered and radial basis function kernel is used. The kernel parameter is selected as average of the mutual distances between the pixels. Unmixing is performed on the data with dimensionality expansion and the corresponding stack of abundance maps are used for classification to validate the effectiveness of the unmixing strategy.

4.3 Classification Results

Table 4.3 and Table 4.3 show the results of classification using various processing chains described in Section 2. It can be observed that the proposed unmixing chain performs better compared to the classification of the multispectral data which is an indirect validation of the unmixing procedure. The addition of the spatial information leads to better characterization of the classes of interest and hence better classification results are obtained.

4.4 Metric to evaluate unmixing

The results of unmixing can be evaluated based on the quality of the reconstruction of the data based on the end-memebers. The metric employed to evaluate the goodness of the reconstruction is the root mean square error (RMSE) obtained in the reconstruction of the expanded image (using the derived endmembers and ther corresponding abundance fractions). This metric is based on the assumption that a set of high-quality endmembers (and their corresponding estimated abundance fractions) may allow reconstruction of the original expanded scene with higher precision compared to a set of low-quality endmembers. In this case, the original

*http://dynamo.ecn.purdue.edu/biehl/MultiSpec

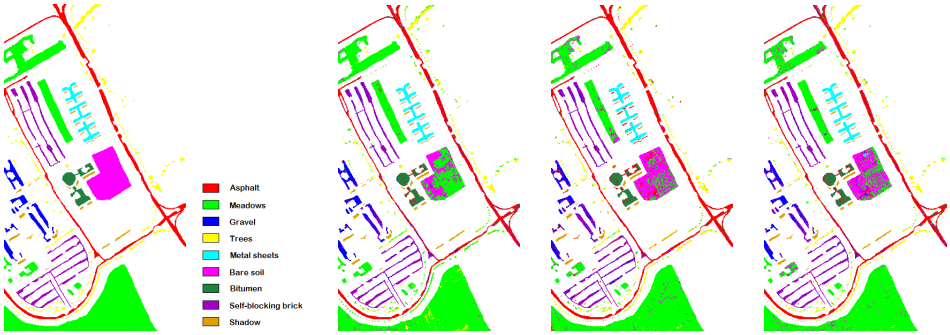

(a) (b) (c) (d)

Figure 4. Classification results for ROSIS PAVIA UNIVERSITY (using SVM classifier trained with 5% of the available samples per class). (a) Ground-truth. (b) Original hyperspectral (83.48%). (c) EMAP(RGB) (85.65%). (d) EMAP(KPCA(RGB)) (86.60%).

Table 2. Overall accuracy (in percentage) and standard deviation obtained after aplying the differents unmixing chains with the SVM classifier for the AVIRIS INDIAN PINES scene.

Overall Accuracy	**AVIRIS INDIAN PINES**		
Features	**5% Training**	**10% Training**	**15% Training**
RGB Multispectral	48.33% ± 0.71	49.63% ± 0.29	49.86% ± 0.38
Original Hyperspectral	**67.71% ± 3.01 (28)**	**71.79% ± 1.88 (28)**	**74.00% ± 2.41 (28)**
EMAP(RGB)	65.49% ± 1.91 (28)	70.74% ± 1.20 (28)	71.85% ± 1.46 (28)
KPCA(RGB)	48.17% ± 0.66 (20)	49.25% ± 0.41 (20)	49.61% ± 0.30 (20)
EMAP(KPCA(RGB))	50.48% ± 1.73 (28)	53.16% ± 1.02 (28)	55.19% ± 0.41 (28)

expanded image is used to measure the fidelity of the reconstructed version of the same scene on a per-pixel basis.

Fig. 6 graphically represents the per-pixel RMSE obtained after reconstructing the different scenes using 13 endmembers (obtained by the Virtual Dimensionality method), extracted by different scenes (original hyperspectral, EMAP (RGB) and EMAP(KPCA(RGB))). It can be seen that the EMAP(RGB) provides better reconstruction error. It is due to the fact that spatial infomation is used. Moreover, the obtained endmembers may not have physical meaning like the spectral endmembers of the hyperspectral data. So it is not possible to directly compare. On the other hand it is interesting to note that the unmixing of EMAP of KPCA features does not provide a good unmixing result. This might be due to the fact that KPCA is a non-linear method and only linear unmixing is used in this work. Similar patter is observed for the AVIRIS data as shown in Fig. 7.

5. CONCLUSION AND FUTURE LINES

This paper has described a new framework for spectral unmixing of multispectral remote sensing images with limited spectral resolution, only a few bands spectral. Extended Multi-Attribute Attribute Profiles (EMAPs) have been introduced for expanding the dimensionality of RGB images. EMAPs provide a huge dimensionality of data to facilitate the usage of unmixing algorithms developed for spectral unmixing. It is difficult to interpret

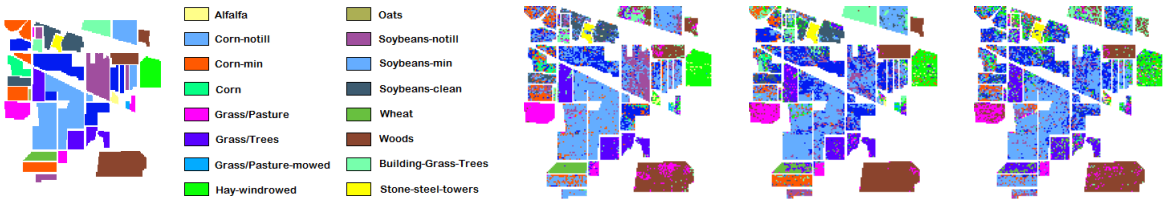

(a) (b) (c) (d)

Figure 5. Classification results for AVIRIS INDIAN PINES (using SVM classifier trained with 5% of the available samples per class). (a) Ground-truth. (b) Original hyperspectral (67.71%). (c) EMAP(RGB) (65.49%). (d) EMAP(KPCA(RGB)) (50.48%).

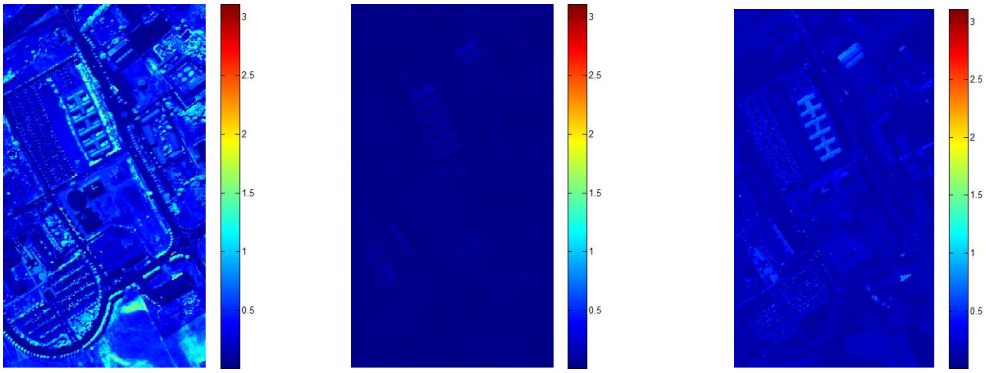

Orig. Hyperspectral (RMSE=0.4000) EMAP(RGB) (RMSE=0.0305) EMAP(KPCA_n1p0(RGB)) (RMSE=0.1765)

Figure 6. RMSE reconstruction errors (with the RMSE average value in the parenthesis) for different chains of unmixing after reconstructing the ROSIS PAVIA UNIVERSITY scene using morphological attributes with the SVM classifier.

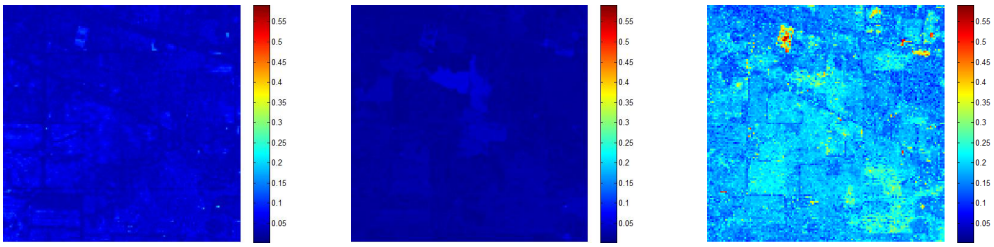

Orig. Hyperspectral (RMSE=0.0445) EMAP(RGB) (RMSE=0.0200) EMAP(KPCA(RGB)) (RMSE=0.1814)

Figure 7. RMSE reconstruction errors (with the RMSE average value in the parenthesis) for different chains of unmixing after reconstructing the AVIRIS INDIAN PINES scene using morphological attributes with the SVM classifier.

the obtained endmembers, as they may not have any physical significance unlike the spectral endmembers. However, experiments show that significant improvements in classification results can be obtained using this processing strategy on the EMAPs built using multispectral images. In the future we would like to study the correspondence of the obtained endmembers to the spatial properties of the objects in the image. The low reconstruction error suggest that correct end-members are identified using the proposed unmixing chain. The dimensionality expansion using KPCA however do not yield better results. This might be due to the fact that it is a non-linear method and linear unmixing is considered in this study.

6. ACKNOWLEDGEMENT

This work has been supported by the European Community's Marie Curie Research Training Networks Programme under reference MRTN-CT-2006-035927 (HYPER-I-NET). Funding from the Icelandic Research Council and the Spanish Ministry of Science and Innovation (HYPERCOMP/EODIX project, reference AYA2008-05965-C04-02) is gratefully acknowledged.

REFERENCES

1. A. Plaza, P. Martinez, R. Perez, and J. Plaza, "Spatial/spectral endmember extraction by multidimensional morphological operations," *Geoscience and Remote Sensing, IEEE Transactions on* **40**, pp. 2025 – 2041, sep 2002.
2. M. Zortea and A. Plaza, "Spatial-spectral endmember extraction from remotely sensed hyperspectral images using the watershed transformation," in *Geoscience and Remote Sensing Symposium (IGARSS), 2010 IEEE International*, pp. 963 –966, july 2010.
3. O. Eches, N. Dobigeon, and J.-Y. Tourneret, "Enhancing hyperspectral image unmixing with spatial correlations," *Geoscience and Remote Sensing, IEEE Transactions on* **49**, pp. 4239 –4247, nov. 2011.
4. A. Zare, "Spatial-spectral unmixing using fuzzy local information," in *Geoscience and Remote Sensing Symposium (IGARSS), 2011 IEEE International*, pp. 1139 –1142, july 2011.

5. M. Iordache, J. Dias, and A. Plaza, "Total variation spatial regularization for sparse hyperspectral unmixing (accepted)," *Geoscience and Remote Sensing, IEEE Transactions on* **1**, pp. 1–10, December 2012.
6. A. Villa, J. Chanussot, J. Benediktsson, and C. Jutten, "Spectral unmixing for the classification of hyperspectral images at a finer spatial resolution," *Selected Topics in Signal Processing, IEEE Journal of* **5**, pp. 521 –533, june 2011.
7. M. Dalla Mura, J. A. Benediktsson, B. Waske, and L. Bruzzone, "Morphological attribute profiles for the analysis of very high resolution images," *Geoscience and Remote Sensing, IEEE Transactions on* **48**, pp. 3747 –3762, oct. 2010.
8. M. Dalla Mura, J. A. Benediktsson, B. Waske, and L. Bruzzone, "Extended profiles with morphological attribute filters for the analysis of hyperspectral data," *International Journal of Remote Sensing* **31**(22), pp. 5975–5991, 2010.
9. C.-I. Chang and Q. Du, "Estimation of number of spectrally distinct signal sources in hyperspectral imagery," *IEEE Trans. Geosci. Remote Sens.* **42**(3), pp. 608–619, 2004.
10. J. M. P. Nascimento and J. M. Bioucas-Dias, "Vertex Component Analysis: A Fast Algorithm to Unmix Hyperspectral Data," *IEEE Trans. Geosci. Remote Sens.* **43**(4), pp. 898–910, 2005.
11. D. Heinz and C.-I. Chang, "Fully constrained least squares linear mixture analysis for material quantification in hyperspectral imagery," *IEEE Trans. Geosci. Remote Sens.* **39**, pp. 529–545, 2001.
12. J. A. Benediktsson, J. A. Palmason, and J. R. Sveinsson, "Classification of hyperspectral data from urban areas based on extended morphological profiles," *Geoscience and Remote Sensing, IEEE Transactions on* **43**, pp. 480 – 491, march 2005.
13. P. Soille, *Morphological image analysis: principles and applications*, Springer-Verlag, Berlin, 2003.